

## EFFECTS OF PLASMA SURFACE TA ALLOYING ON THE TRIBOLOGY BEHAVIOR OF $\gamma$ -TiAl

D.-B. Wei <sup>a, b, c\*</sup>, X. Zhou <sup>a, b\*</sup>, F.-K. Li <sup>a, b</sup>, M.-F. Li <sup>a, b</sup>, S.-Q. Li <sup>a, b</sup>, P.-Z. Zhang <sup>a, b</sup>

<sup>a</sup> College of Materials Science and Technology, Nanjing University of Aeronautics and Astronautics, Nanjing, China

<sup>b</sup> Materials Preparation and Protection for Harsh Environment Key Laboratory of Ministry of Industry and Information Technology, Nanjing, China

<sup>c</sup> Aero-engine Thermal Environment and Structure Key Laboratory of Ministry of Industry and Information Technology, Nanjing, China

(Received 17 June 2020; accepted 27 December 2020)

### Abstract

To improve the wear resistance of  $\gamma$ -TiAl alloy, Ta alloy layer was prepared on surface by double glow plasma surface alloying technique. The tribology behavior of Ta alloy layer against  $\text{Si}_3\text{N}_4$  at 25°C, 350°C and 500°C were comparatively studied. The results showed that Ta alloy layer comprised a deposition layer and a diffusion layer. The deposition layer played a role in protection as a soft film. With the increase of temperature, the wear mechanism of  $\gamma$ -TiAl changed from abrasive wear to coexistence of abrasive wear and oxidation wear. Ta alloy layer's wear mechanism changed from adhesive wear to coexistence of adhesive wear and oxidation wear. Surface Ta alloying process significantly reduced the wear volume, the specific wear rate and the friction coefficient of  $\gamma$ -TiAl and improved the wear resistance properties of  $\gamma$ -TiAl.

**Keywords:**  $\gamma$ -TiAl; Plasma surface Ta alloying; Wear resistance; Tribology behavior

### 1. Introduction

$\gamma$ -TiAl alloys are widely used in the automotive, aerospace, and power generation industries with excellent mechanical properties, such as excellent ultimate tensile strength, creep resistance, and high specific modulus [1]. However, there will be a sharp drop in high temperature oxidation resistance of  $\gamma$ -TiAl above 700°C. This could be attributed to the loose structure of  $\text{TiO}_2$ - $\text{Al}_2\text{O}_3$  composite oxide film on the surface, reducing its compactness and decreasing its mechanical resistance. As a result, high-temperature oxidation resistance of  $\gamma$ -TiAl alloys could be reduced [2, 3]. Moreover, the brittleness and low surface hardness of  $\gamma$ -TiAl could lead to reduced wear resistance at room temperature. At high temperature, the flaky oxide film, which is relatively easy to peel off, does not play a role in protecting the surface, and even exposes the surface, aggravating the degree of wear. The weaknesses could not be ignored, and could vastly limit the application at high temperature. Kazuhisa Miyoshi found that wear in the turbine engine reduced the service life, especially high temperature wear [4-6]. This could be attributed to a fact that during the use of the dovetail, metal surfaces inevitably came into contact, and high temperature wear was liable to occur under the load and high temperature, which was the potential

safety hazard to the turbine engine (Fig.1). Therefore, it was necessary to improve the high-temperature oxidation and wear resistance of  $\gamma$ -TiAl for its broader implications, especially in the aerospace industry.

Adding alloying elements, such as Cr, Y, Mo, Si, and Nb was proved to be an effective method to improve both the high-temperature oxidation resistance and the wear resistance of  $\gamma$ -TiAl. However, some studies have shown that when the amount of Cr and Y in the  $\gamma$ -TiAl is insufficient, the improvement

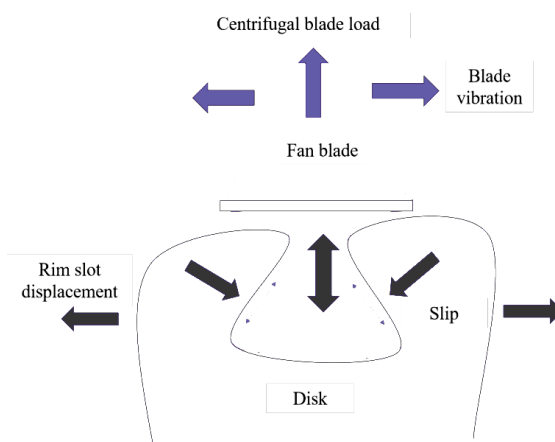


**Figure 1.** Schematic diagram of wear at the dovetail

\*Corresponding author: weidongbo@nuaa.edu.cn; zx940620@nuaa.edu.cn

disappears with the increase of oxidation time [7]. After adding Mo, the  $\text{TiO}_2$  layer was still maintained, and the as-gained oxidation weight of the alloy was still evident, with the addition of the oxidation time [8]. When  $\gamma$ -TiAl contained too much Si, the brittleness could increase and the wear resistance decreased. But, in fact it is not enough for the formation of a continuous  $\text{Al}_2\text{O}_3$  protective layer on the surface of  $\gamma$ -TiAl even when the Nb element content is as high as 10 at% [9]. In the periodic table, Ta was close to the position of Nb, which was expected to induce similar properties as Nb in the process of high-temperature oxidation. Initial studies suggested that Ta hindered the oxidation process, but not as much as Nb. Therefore, Ta was regarded as a neutral in high-temperature oxidation or even ignored. Recent studies showed that Ta could efficiently optimize the structure and mechanic resistance of  $\gamma$ -TiAl at room temperature [10-12]. Some references even pointed out that Ti46Al8Ta (without Nb) could be a part of the fourth-generation TiAl alloys, which was used as the engine blade material in Europe [13]. Chinese institutes successfully prepared high-temperature alloy TiAl-3Ta-X(Cr,W), and successfully enhanced the high-temperature oxidation resistance. The research results showed that the alloy formed a square  $\text{AlTaO}_4$  phase during the oxidation processes, which efficiently prevented spreading O from the surface to the interior, thus inhibiting the oxidation of the alloy [14].

Ta's effect on  $\gamma$ -TiAl, especially on the high temperature oxidation, is focused on by lots of researches. High-temperature oxidation mainly occurred on the surface of the alloy. In comparison with adding Ta to the  $\gamma$ -TiAl alloy, surface alloying with Ta could be a cost-efficient method to control the alloying degree [15,16]. Double glow plasma surface alloying technology (DG) provided an alternative approach for surface alloying with Ta on  $\gamma$ -TiAl [17]. The principle of double glow plasma surface alloying technology was to achieve the alloying of the surface

of the material by using low-temperature plasma generated by glow discharge under vacuum condition. In recent years, Ni, Cr, Mo, W, and Cu were successfully alloyed on the surface of pure iron, carbon steel, titanium, and titanium alloys by double glow plasma surface alloying technology. It has improved the corrosion resistance, wear resistance, high temperature oxidation resistance and other properties of the material on varying degree. The schematic diagram and experimental photograph of DG were shown in Fig.2 [18-20].

In our previous studies, we had successfully obtained alloy with Ta on the surface of  $\gamma$ -TiAl by double glow plasma surface alloying technology and investigated its high-temperature oxidation behavior [21]. The results showed that Ta facilitated the diffusion of Al, forming a uniformly mixed  $\text{Al}_2\text{O}_3/\text{Ta}_2\text{O}_5$  film. Meanwhile, Ta prevented the inward diffusion of O, which helped to improve the high-temperature oxidation resistance.

As previously described, not only did high temperature risks need to be considered, but wear was another issue that needs to be addressed, especially at high temperature. In this work, the wear resistance of  $\gamma$ -TiAl after plasma surface Ta alloying at different temperatures was investigated. The ball-on-disc friction and wear test sliding against  $\text{Si}_3\text{N}_4$  was carried out at 25°C, 350°C and 500°C. The friction coefficient, wear volume and specific wear rate were studied, and the wear mechanism was analyzed.

## 2. Experimental

### 2.1. Experiment materials

The chemical composition of  $\gamma$ -TiAl was shown in Table 1. The specimens were cut into square samples (15mm×15mm×4mm). The surface was mechanically polished with a Ra<0.1  $\mu\text{m}$  diamond paste, cleaned with acetone, and dried. The source material for Ta target (100 wt.%), made of the powder metallurgy

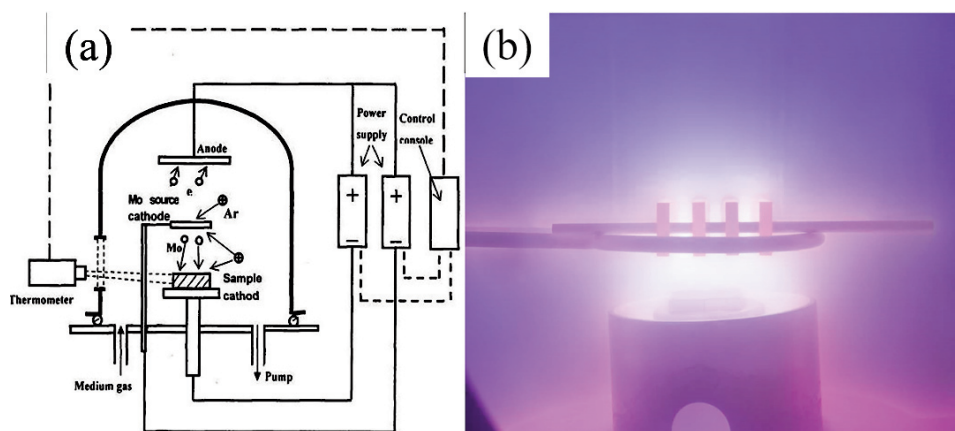


Figure 2. Schematic diagram and experimental photograph of DG; (a) Schematic diagram (b) experimental photograph



method, was cylindrical ( $\phi 100$  mm,  $d5$  mm). The working gas was argon, which had strong sputtering ability and strong inertia. Parameters of double glow plasma surface Ta alloying were shown in Table 2.

**Table 1.** Chemical composition of  $\gamma$ -TiAl (wt.%)

Ti	Al	V	Cr	Nb	O	C	N
Bal.	46.5	$\leq 1.5$	$\leq 1$	$\leq 0.20$	$\leq 0.015$	$\leq 0.10$	$\leq 0.05$

**Table 2.** Parameters of double glow plasma surface Ta alloying

Voltage of the source / V	Voltage of the substrate / V	Working pressure / Pa	Distance / mm	Time/h
900	500	35	20	3.5

## 2.2. Materials characterization

The surface morphology and cross-section morphology of Ta alloy layer were observed by a scanning electron microscope (SEM). The chemical composition was performed by X-ray diffraction (XRD) and energy dispersive X-ray spectrometry (EDS).

## 2.3. Hardness

The hardness of Ta alloy layer was measured employing a Micro vickers hardness machine (HXS-100A) with 100g load and loading 10s. The result of the measurement was the average of five different dots, in order to characterize the uniformity of the layer's surface hardness and ensured the accuracy.

## 2.4. Friction and wear test

The treated samples and untreated samples were subjected to friction and wear test using ball-on-disc tribometer (HT-500) at 25°C, 300°C and 500°C. Test was performed at 470 g normal load and sliding speed was 560 rpm with 15 min. The counterpart ball was

made of  $\text{Si}_3\text{N}_4$ , diameter of which was 4.5 mm. The surface profile was characterized by surface profiler. Due to different densities between  $\gamma$ -TiAl and Ta, it was unsuitable to use the weight loss to characterize the wear of the samples. The weight loss was counted through the depth and width of the wear scar, presenting below [19].

$$W = Lh(3h^2 + 4b^2) / (6b) \quad (1)$$

Where  $W$  was the weight loss (mm),  $L$  was the wear scar length,  $h$  was the depth of wear scar and  $b$  was the width of wear scar.

In this way, the specific wear rate was calculated through dividing the wear volume by the load and sliding distance, presenting below.

$$K = V / PS \quad (2)$$

Where  $K$  was the specific wear rate ( $\text{mm}^3\text{N}^{-1}\text{m}^{-1}$ ),  $V$  was the wear volume ( $\text{mm}^3$ ),  $P$  was the load (N) and  $S$  was the total sliding distance (m).

## 3. Results

### 3.1 Microstructure characterization of Ta alloy layer

Fig.3 showed the surface morphology and composition analysis diagram of Ta alloy layer. As could be seen from Fig.3(a), Ta alloy layer was uniform, compact, and had no cracks or holes. A large number of silver-white particles were dispersed on the surface, with similar size and uniform distribution. The  $\gamma$ -TiAl's surface completely was covered by the alloy layer, and the Ta element accounted for 100% of Ta alloy layer. Fig.3(b) showed the XRD pattern of the Ta alloy layer. The diffraction peaks at  $38.25^\circ$  and  $68.75^\circ$  were assigned to the (110) and (211) planes of the body-centered cubic  $\alpha$ -Ta.

Fig.4 showed the cross-section morphology and composition analysis diagram of the Ta alloy layer. It could be observed that the Ta alloy layer was mainly composed of a deposition layer and a diffusion layer, which is observable in Fig.4(a). The deposition layer had

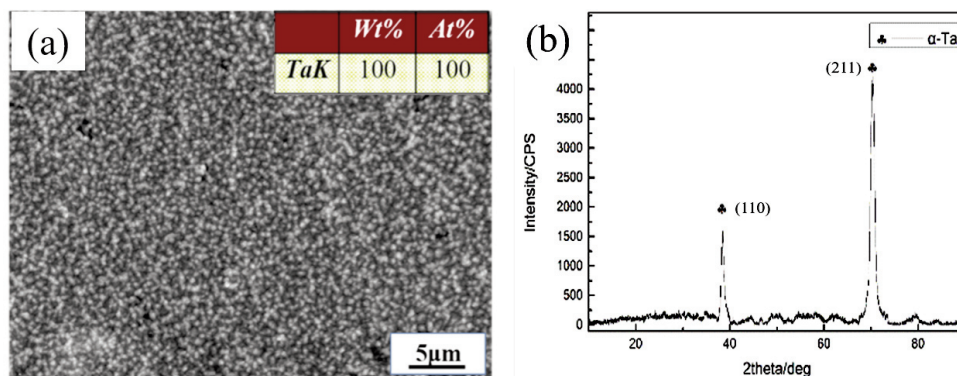


**Figure 3.** Surface morphology and XRD pattern of Ta alloy layer (a) surface morphology (b) XRD pattern

a thickness of about 10  $\mu\text{m}$ , and the thickness of diffusion layer was about 3  $\mu\text{m}$ . The interface was not smooth, but the structure was dense and had no cracks. Fig.4(b) showed that Ta descended from the outside-in, while Ti and Al rose. It indicates that Ti and Al diffuse into the alloy layer when Ta diffuses into the surface. The diffusion layer is formed in this process, strengthening the binding force which shows the advantages of double glow plasma surface alloying technology.

### 3.2 Mechanical properties

#### 3.2.1. Hardness

$\gamma$ -TiAl showed a hardness of about Hv 318.3. By contrast, the Ta alloy layer had a hardness value of Hv 775.9 approximately. It could be expected that the

hardness value of the Ta alloy layer was higher than  $\gamma$ -TiAl, due to the solution strengthening effect caused by the infinite solid solution between Ta and  $\beta$ -Ti.

#### 3.2.2. Friction and wear test

The friction coefficient curves of the  $\gamma$ -TiAl and Ta alloy layers at different temperatures were shown in Fig.5. The friction coefficients of  $\gamma$ -TiAl were 0.72, 0.88, and 0.96 at 25°C, 350°C, and 500°C, respectively. The friction coefficients of the Ta alloy layer were 0.51, 0.63, and 0.71 at 25°C, 350°C, and 500°C, respectively. The plastic shearing was mainly responsible for the friction coefficients of the Ta alloy layer and  $\gamma$ -TiAl add radically from 0. After the running-in stage of 2 min, the curve tends to be stable. It could also be seen that the average friction

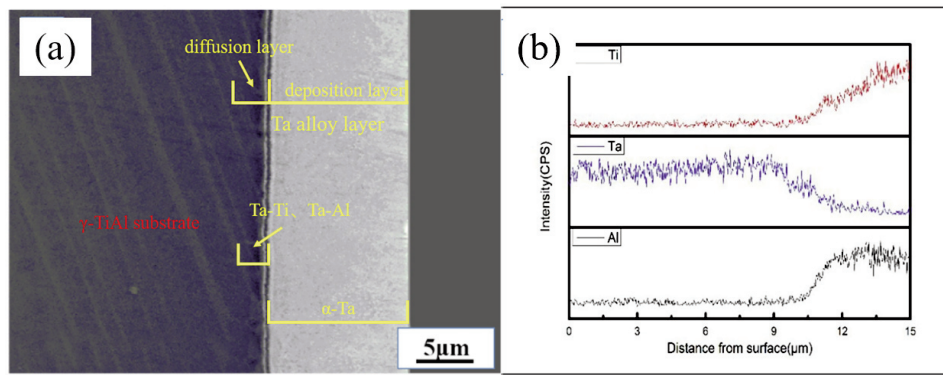


Figure 4. Cross-sectional morphology and composition analysis diagram of Ta alloy layer: (a) cross-sectional morphology (b) component distribution

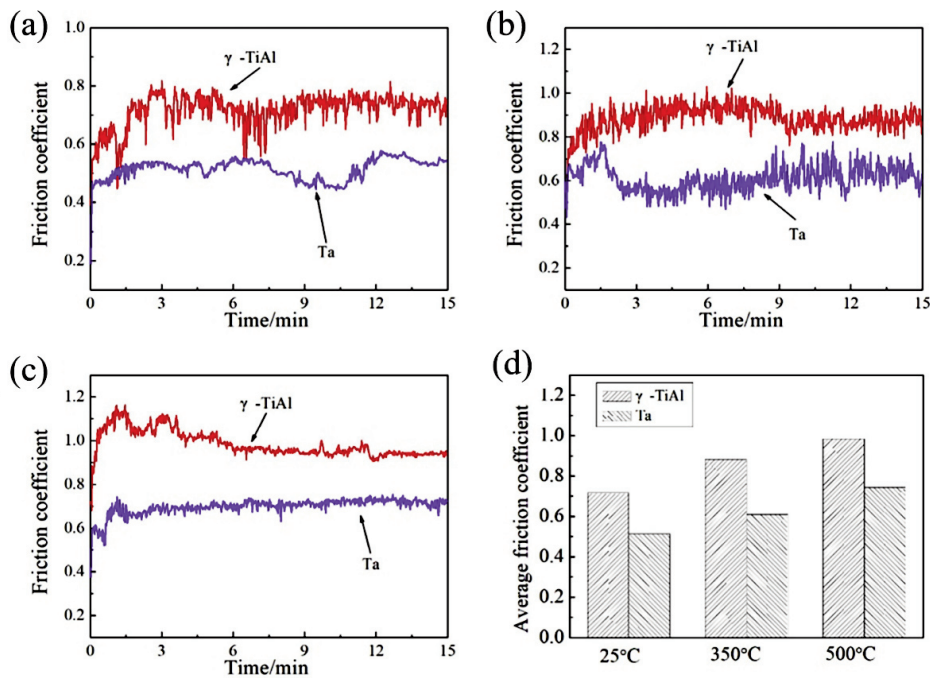


Figure 5. Friction coefficient curves of  $\gamma$ -TiAl and Ta alloy layer (a) 25°C (b) 350°C (c) 500°C (d) average friction coefficient

coefficients of  $\gamma$ -TiAl and Ta alloy layers were increased with the increasing temperature, and the friction coefficients of the Ta alloy layer were lower than those obtained in the case of  $\gamma$ -TiAl.

Fig.5(a) showed that the friction coefficient curve of  $\gamma$ -TiAl fluctuated significantly at 25°C, while the fluctuation of the friction coefficients in the case of Ta alloy layer was smaller. Fig.6 showed the wear scar morphology of the  $\gamma$ -TiAl and Ta alloy layer at 25°C. The comparison of Fig.6(a) and (c) revealed that the wear scar morphology of  $\gamma$ -TiAl presented many furrows paralleled to the sliding direction, accompanied by debris and no adhesion phenomenon observed. There was a typical feature of abrasive wear. The wear scar morphology of the Ta alloy layer showed apparent signs of tear. There was a typical feature of adhesive wear, as at the middle part of the scar was interlaced with silvery-white and dark particle. EDS analysis showed that the white area mainly consisted of Ta oxides. Fig.5(b) showed that the fluctuation range of friction coefficient of  $\gamma$ -TiAl at 350°C was smaller than that at 25°C. Meanwhile, that of the Ta alloy layer had an increment at 350°C. Fig.6 showed the wear scar morphology of the  $\gamma$ -TiAl and Ta alloy layer at 350°C. Compared to Fig.7(a) and (c), there were still lots of severe furrows and many pieces of debris on  $\gamma$ -TiAl. A large number of silver-white particles were distributed on the surface of the wear. It could also be observed that there was a decrease of disruption and plastic deformation and an increase of debris on Ta alloy layer. In the friction process, the oxides were produced on the surface of  $\gamma$ -TiAl and the Ta alloy layer. Fig.5(c) showed the fluctuation of friction coefficient of  $\gamma$ -TiAl and Ta alloy layer gradually. Fig.8 showed the wear scar morphology of the  $\gamma$ -TiAl and Ta alloy layer at 500°C. It was also found that the wear scar morphology of  $\gamma$ -TiAl still presented many furrows, accompanied by tear phenomenon (Fig.8(a)). Compared with EDS analysis at 350°C, the degree of oxidation intensified.

The wear scar morphology of the Ta alloy layer showed visible characteristics of adhesive wear (Fig.8(c)). Plastic deformation and adhesion phenomena were appearing on the surface without furrows. As the temperature increased, the oxidation degree increased as well, and the presence of the oxide film protected the  $\gamma$ -TiAl alloy.

Fig.9 showed the surface profiles of wear tracks of  $\gamma$ -TiAl before and after alloying the surface with Ta, at different temperatures. Table 3 showed the values of wear scar width, wear scar depth, and wear volume of  $\gamma$ -TiAl and Ta alloy layer at different temperatures. The wear volume was measured by equation (1). It was shown that the wear volume of the Ta alloy layer was much smaller than that of  $\gamma$ -TiAl. As the temperature increased, the wear volume of the  $\gamma$ -TiAl and Ta alloy layers showed a varying degree. The specific wear rates of  $\gamma$ -TiAl were  $72.544 \times 10^{-6} \text{mm}^3 \text{N}^{-1} \text{m}^{-1}$ ,  $114.267 \times 10^{-6} \text{mm}^3 \text{N}^{-1} \text{m}^{-1}$ , and  $159.804 \times 10^{-6} \text{mm}^3 \text{N}^{-1} \text{m}^{-1}$  at 25°C, 350°C, and 500°C, respectively. The specific wear rates of the Ta alloy layer were  $11.732 \times 10^{-6} \text{mm}^3 \text{N}^{-1} \text{m}^{-1}$ ,  $16.671 \times 10^{-6} \text{mm}^3 \text{N}^{-1} \text{m}^{-1}$ , and  $27.834 \times 10^{-6} \text{mm}^3 \text{N}^{-1} \text{m}^{-1}$  at 25°C, 350°C, and 500°C, respectively.

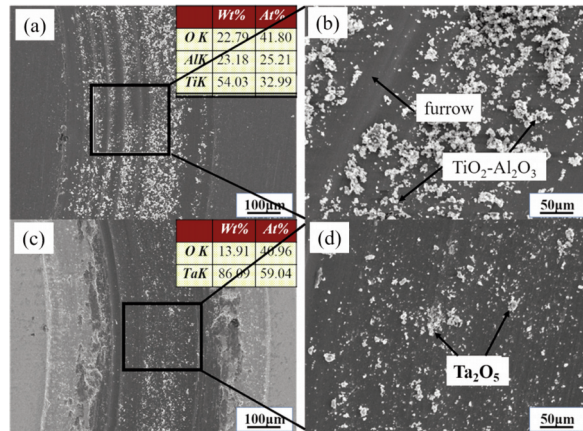


Figure 7. Wear scar morphology of  $\gamma$ -TiAl and Ta alloy layer at 350°C: (a)(b)  $\gamma$ -TiAl (c)(d) Ta alloy layer

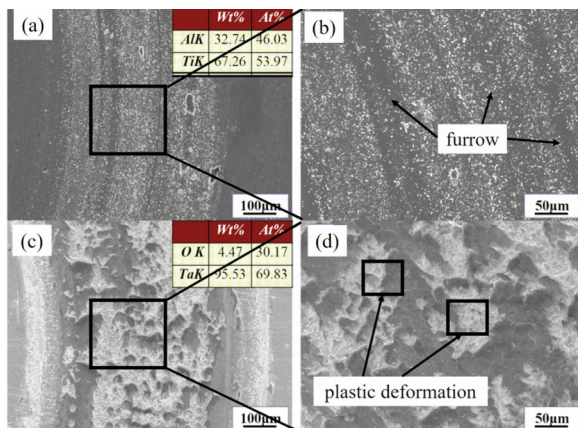


Figure 6. Wear scar morphology of  $\gamma$ -TiAl and Ta alloy layer at 25°C: (a)(b)  $\gamma$ -TiAl (c)(d) Ta alloy layer

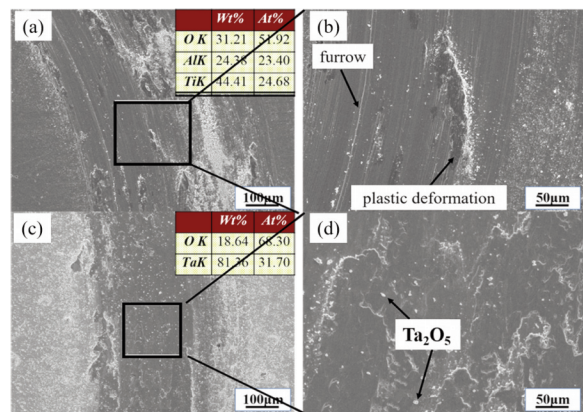


Figure 8. Wear scar morphology of  $\gamma$ -TiAl and Ta alloy layer at 500°C: (a)(b)  $\gamma$ -TiAl (c)(d) Ta alloy layer



**Table 3.** Wear dates of  $\gamma$ -TiAl and Ta alloy layer at 25°C, 350°C and 500°C

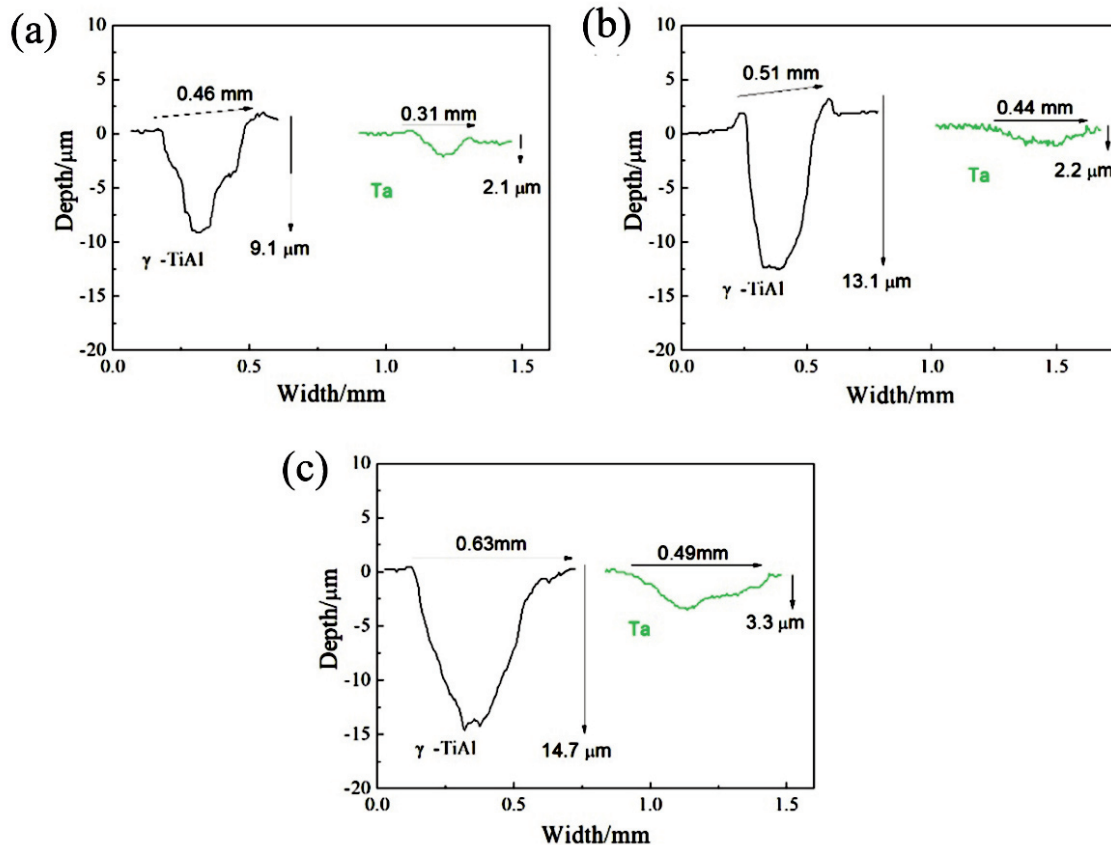
Temperature / °C	Specimens	Wear scar width / mm	Wear scar depth / $\mu\text{m}$	Wear volume / $10^{-3}\text{mm}^3$
25°C	$\gamma$ -TiAl	0.466	9,146	35,728
	Ta alloying	0.317	2,183	5,799
350°C	$\gamma$ -TiAl	0.512	13,139	56,401
	Ta alloying	0.443	2,204	8,194
500°C	$\gamma$ -TiAl	0.638	14,746	78,927
	Ta alloying	0.493	3,331	13,760

#### 4. Discussion

Ball-on-disc friction and wear test indicated that the friction coefficient of the alloy layer was smaller than that of  $\gamma$ -TiAl at different temperatures. The reason could be that the lower surface roughness of  $\gamma$ -TiAl increased the actual contact area, resulting in the augmentation of surface molecular attraction. As the temperature increased, the fluctuation of friction coefficient of  $\gamma$ -TiAl and Ta alloy layer leveled off, because while

the temperature increased, the oxidation film produced on the surface had the effect of lubrication. In the other's finding [22], they believed that at high temperature the yielding strength of  $\gamma$ -TiAl, Ta alloy and  $\text{Si}_3\text{N}_4$  decreased and the plasticity of that increased. Therefore, with the increase of temperature, the friction coefficient fluctuation of  $\gamma$ -TiAl and Ta alloy layer could tend to flat gradually.

Under the action of load, the surface of  $\gamma$ -TiAl formed debris, due to low hardness. The debris cut the surface with loading and formed furrows. As the temperature increased, the number of debris cut from the surface increased, similar to the number and depth of the furrows. At high temperatures, an increased adhesion between the  $\text{Si}_3\text{N}_4$  and  $\gamma$ -TiAl was observed, resulting in a degree of plastic deformation and disruption. The wear scar morphology of Ta alloy layer presented a typical feature of plastic deformation, mainly due to the fact that there was the deposition layer of loose stacking structure, which had good plastic deformation ability. Under the load, it appeared the adhesive wear between the deposition layer and the mill balls. As a soft film, the oxide film on surface played a lubricative role. However, under the long-term

**Figure 9.** Surface profiles of wear tracks of  $\gamma$ -TiAl and Ta alloy layer (a) 25°C (b) 350°C (c) 500°C

action of load, the integrity of the oxide film could not be maintained, and formed granular debris. Along with the destruction and regeneration of the oxide film, the oxidation of  $\gamma$ -TiAl and Ta alloy layer changed dynamically, which further aggravated the wear degree. The number of oxidation particles on  $\gamma$ -TiAl was more than that of Ta alloy layer, indicating that Ta alloy layer had better high temperature oxidation resistance and formed an oxide film of stable structure. It is consistent with the experimental results of Ta alloy layer at high temperature oxidation. When the temperature increased, the wear mechanism of  $\gamma$ -TiAl changed from abrasive wear to coexistence of abrasive wear and oxidative wear. Meanwhile, the wear mechanism of the Ta alloy layer changed from adhesive wear to coexistence of oxidative wear and adhesive wear.

The wear depth and width of the Ta alloy layer was lower than that of  $\gamma$ -TiAl, due to the higher hardness value of the Ta alloy layer, as it was difficult to break the surface under the cutting action of load. It could also be seen that the wear depth and width of the treated sample was much lower than that of the untreated sample. This was following the analysis showing that the wear mechanism of the alloy layer was mainly adhesive wear. Compared with the wear volume and the specific wear rate of the  $\gamma$ -TiAl and Ta alloy layer, it could be seen that the most significant proportion was presented at 25°C when the wear volume of the Ta alloy layer was 23.8 % of  $\gamma$ -TiAl. This is attributed to the formation of oxidation film on the surface at high temperature, playing a lubricating effect and reducing wear. It was the most significant proportion at 500°C that the specific wear rate of the Ta alloy layer was 23.8 % of  $\gamma$ -TiAl.

## 5. Conclusions

The samples before and after double glow plasma surface Ta alloying were investigated to evaluate the wear resistance at 25°C, 350°C and 500°C. The conclusions derived from this paper are summarized as follows:

(1) Ta alloy layer was uniform and compact and had no holes. It included the deposition layer of 10 $\mu$ m and the diffusion layer of 3 $\mu$ m, of which the combination was better.

(2) A ball-on-disc friction and wear test indicated that there was a significant decrease of the wear volume, the specific wear rate, and the friction coefficient of  $\gamma$ -TiAl after double glow plasma surface Ta alloying process. Deposition layer played a role in reducing the friction and lubricating as soft film.

(3) As the temperature increased, the  $\gamma$ -TiAl wear mechanism changed from abrasive wear to

coexistence of abrasive wear and oxidation wear. Besides, the wear mechanism of Ta alloy layer changed from adhesive wear to coexistence of adhesive wear and oxidation wear. From the above, it could be concluded that the Ta alloy layer obtained by DG improved the wear resistance of  $\gamma$ -TiAl efficiently.

## Acknowledgments

*This project was supported by Natural Science Foundation for Excellent Young Scientists of Jiangsu Province, China (Grant No. BK20180068), China Postdoctoral Science Foundation funded project (Grant No. 2018M630555), Opening Project of Materials Preparation and Protection for Harsh Environment Key Laboratory of Ministry of Industry and Information Technology (Grant No. XCA20013-1).*

## 5. References

- [1] Shi, X.L, Xu, Z.S, Wang, M, Zhai, W.Z, Yao, J, Song, S.Y, *Wear*, 303(1-2) (2013) 486-494.
- [2] M.P. Brady, W.J. Brindley, J.L. Smialek, *JOM*, 48(11) (1996) 46-50.
- [3] A. Gil, H. Hoven, E. Wallura, W. Quadackers, *J. Cor. Sci.*, 34(4) (1993) 615-630.
- [4] K. Miyoshi, B.A. Lerch, *S.L. Tri. Int.*, 36(2) (2003) 145-153.
- [5] T. Hansson, M. Kamaraj, Y. Mutoh, *Ast.m Spec. Tech. Publ.* 1367 (1998) 15.
- [6] S. Chakravarty, R.G. Andrews, P.C. Patnaik, A.K. Koul, *JOM*, 47(4) (1995) 31-35.
- [7] Y. Shida, H. Anada, *Oxid. Met.*, 45(1-2) (1996) 197-219.
- [8] D. Caillard, A. Couret, *Microsc. Res. Tech.*, 72(3) (2009) 261-269.
- [9] A. Ismaeel, C.S. Wang, *T. Nonferr. Metal. Soc.*, 29(5) (2019) 1007-1016.
- [10] H. Fang, R. Chen, X. Chen, *Int.*, 104 (2019) 43-51.
- [11] M.H. Loretto, Z. Wu, M.Q. Chu, H. Saage, D. Hu, *Int*, 23 (2012) 1-11.
- [12] H. Jiang, K. Zhang, X.J. Hao, H. Saage, *Int*, 18(5) (2010) 938-944.
- [13] H. Saage, A.J. Huang, D. Hu, *Int.*, 17 (1) (2009) 0-38.
- [14] T. Popela, D. Vojtech, J.B. Vogt, *Appl. Surf. Sci.*, 307(15) (2014) 579-588.
- [15] J. Lapin, T. Pelachová, M. Dománková, *Int.*, 19(6) (2011) 0-819.
- [16] T. Izumi, T. Yoshioka, S. Hayashi, *Int.*, 13(7) (2005) 694-703.
- [17] Z.K. Qiu, P.Z. Zhang, D.B. Wei, *Surf. Coat. Tech.*, 278 (2015) 92-98.
- [18] *Surf. Coat. Tech.*, 278 (2015) 92-98.
- [19] D.B. Wei, P.Z. Zhang, Z.J. Yao, *Appl. Surf. Sci.*, 388(1) (2016) 571-578.



- [20] Y. Wang, P. Zhang, H. Wu, D. Wei, X. Wei, P. Zhou, Tribol. T., 57(5) (2014) 786-792. [22] F. Cheng, J. Lin, Y.F. Liang, Intermetallics, 106 (2019) 7-12.
- [21] D.B. Wei, P.Z. Zhang, Y. Yuqin, Oxid. Met., 92(3) (2019) 337-351.

## EFEKTI POVRŠINSKOG LEGIRANJA PLAZMOM Ta NA TRIBOLOŠKO PONAŠANJE $\gamma$ -TiAl

D.-B. Wei <sup>a, b, c\*</sup>, X. Zhou <sup>a, b\*</sup>, F.-K. Li <sup>a, b</sup>, M.-F. Li <sup>a, b</sup>, S.-Q. Li <sup>a, b</sup>, P.-Z. Zhang <sup>a, b</sup>

<sup>a</sup> Fakultet za nauku o materijalima i tehnologiju, Univerzitet za aeronautiku i astronautiku u Nanđingu, Nanđing, Kina

<sup>b</sup> Glavna laboratorija za pripremu i zaštitu materijala koji se koriste u surovim uslovima Ministarstva industrije i informacione tehnologije, Nanđing, Kina

<sup>c</sup> Glavna laboratorija Ministarstva industrije i informacione tehnologije za termičku okolinu i strukturu vazduhoplovnih motora, Nanđing, Kina

### Apstrakt

Da bi se poboljšala otpornost na habanje  $\gamma$ -TiAl legure, površinski sloj Ta legure je pripremljen tehnikom legiranja duplim mlazom plazme. Uporedo je ispitivano tribološko ponašanje sloja Ta legure u poređenju sa  $Si_3N_4$  pri 25°C, 350°C i 500°C. Rezultati su pokazali da je sloj Ta legure obuhvatao depozitni i difuzni sloj. Depozitni sloj je kao mekana prevlaka imao ulogu u zaštiti. Sa porastom temperature, mehanizam habanja  $\gamma$ -TiAl menjao se od abrazivnog habanja do istovremenog postojanja abrazivnog i habanja kao posledice oksidacije. Mehanizam habanja sloja Ta legure menjao se od adhezivnog habanja do istovremenog postojanja adhezivnog habanja i habanja kao posledice oksidacije. Proces legiranja površine sa Ta značajno je smanjio obim habanja, specifičnu stopu habanja, i koeficijent trenja  $\gamma$ -TiAl, i poboljšao otpornost na habanje.

**Ključne reči:**  $\gamma$ -TiAl; Površinsko legiranje plazmom Ta; Otpornost na habanje; Tribološko ponašanje

